Journal of Thermal Analysis, Vol. 45 (1995) 1313-1322

THERMAL BEHAVIOUR OF CO_2 LASER-IRRADIATED CeO_2 DOPED WITH Yb_2O_3

V. I. Pârvulescu[1], *F. Vasiliu*[2] *and E. Segal*[3]*

[1]Research and Engineering Institute for Non-ferrous Metals, B-dul Biruintei 102, Sector 3, Bucharest 7395, Roumania
[2]Research Institute of Materials for Airplanes, Bucharest-Magurele, Roumania
[3]University of Bucharest, Faculty of Chemistry, Department of Physical Chemistry, B-dul. 13, Bucharest 7003, Roumania

(Received January 28, 1995)

Abstract

Results concerning the thermal behaviour of Yb_2O_3-doped CeO_2 samples irradiated with CO_2 laser beams in continuous wave are presented.

Keywords: CeO_2, laser irradiation, Yb_2O_3-doped CeO_2

Introduction

One of the branches of radiation chemistry which have undergone rapid development in recent years is laser chemistry. Within the framework of this, reactions in the gas, liquid and solid states, and also reactions of adsorbed species have been investigated [1].

For reactions that require energetic conditions, CO_2 laser sources have been used. Among such reactions, mention should be made of the pyrolyses of gaseous reactants [2] and the syntheses of ultrafine oxide powders [3, 4].

Some of our previous work has been dedicated to the changes induced by CO_2 laser radiation (continuous wave) on rare earth powders [5, 6]. Derivatographic analyses and electron microscopic investigations demonstrated that samples of CeO_2 powders irradiated with energy densities higher than 6 $kJ \cdot cm^{-2}$ exhibit a structure with nonstoichiometric phases. Subsequent calcination of irradiated samples determines further non-stoichiometrization, showing that some of the irradiation-induced phases are metastable.

* To whom the correspondence should be addressed

0368–4466/95/ $ 5.00

John Wiley & Sons, Limited
Chichester

In this paper, an analysis of the changes induced by CO_2 laser irradiation in samples of powdered CeO_2 doped with 5 wt.% Yb_2O_3 is presented.

Experimental

Samples of CeO_2 with 5 wt.% Yb_2O_3 were synthesized by coprecipitation from cerium nitrate (99.9%) and ytterbium chloride (obtained from ytterbium oxide (Fluka) and hydrochloric acid (Merck) with ammonia solution (Merck)). The precipitate was washed to remove Cl^- and NO_3^- and then dried at 80°C for 4 h and at 105°C for 4 h.

The dried samples were submitted to CO_2 laser irradiation in continuous wave at energy densities in the range 7–15 kJ·cm^{-2} with laser equipment previously described [5]. Before irradiation, the samples were ground to particle sizes lower than 30 μm. The irradiation was performed on layers with a thickness of 1 mm.

The heating curves in the temperature range 25–1000°C were recorded in static air atmospheres with a MOM (Budapest) Paulik-Paulik-Erdey Q 1500-D derivatograph at a heating rate of 10 deg·min^{-1}. As reference material for DTA, samples of CeO_2–Yb_2O_3 calcined at 1000°C were used.

For evaluation of the nonisothermal kinetic parameters of the thermal decomposition in the framework of the reaction order model, three methods were applied: those of Coats-Redfern [7], Flynn-Wall [8] and Urbanovici-Segal [9] (modified Coats-Redfern method). The experimental data were processed by means of a program written in BASIC language [10] and run on a TIM-s computer. The same program allowed regeneration of the TG curves in coordinates (α, t, °C) (α = degree of transformation) using the values of the nonisothermal kinetic parameters and fitting of the experimental points.

The powders of CeO_2–Yb_2O_3 were investigated through transmission electron microscopy (TEM) and selected area electron diffraction (SAED), using JEM – 200 CX electronic microscope. Special precautions were taken to protect the samples from water vapour contamination and to prevent significant temperature increases during the experiments [6].

Results

Thermal analysis data

The heating curves of all of the investigated samples exhibit no weight changes in the temperature range 25–100°C.

Figures 1–3 show heating curves of CeO_2–Yb_2O_3 samples submitted to irradiation for 7 s at energy density values of 7.18, 10.77 and 16.15 kJ·cm^{-2}. The increase of the energy density determines the increase in the mass loss, which does not exceed 2%.

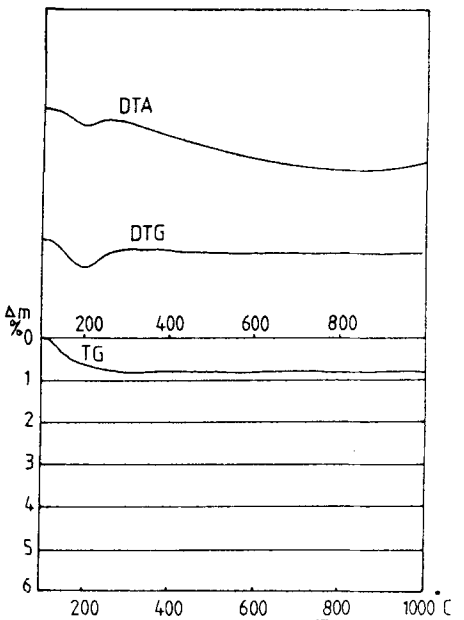

Fig. 1 Heating curves of CeO_2–5 wt.% Yb_2O_3 irradiated for 7 s and energy density of 7.18 kJ·cm^{-2}

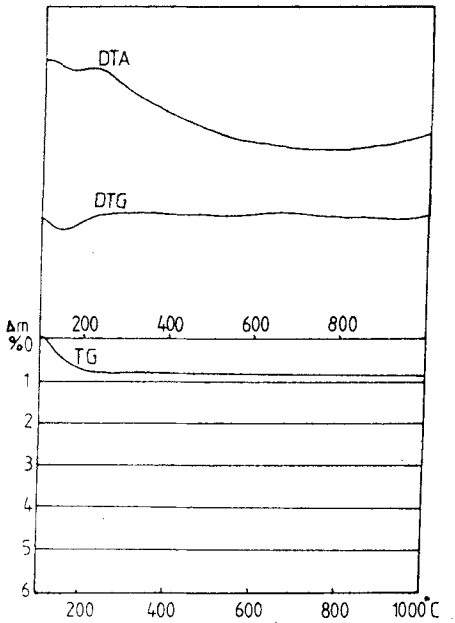

Fig. 2 Heating curves of CeO_2–5 wt.% Yb_2O_3 irradiated for 7 s and energy density of 10.77 kJ·cm^{-2}

Doubling of the exposure time to 14 s under the same working conditions determines the increase in mass loss up to 7.2% at a radiation energy density of 16.15 kJ·cm^{-2} (Figs 4–6).

At low energy densities (Fig. 4), the recorded thermal curves are similar to those recorded at low exposure times and high energy densities (Fig. 3). At high exposure times, increase of the energy density determines more complex heating curves (new peaks in the temperature range 250–450°C). Under such conditions, the loss in mass no longer occurs in a single step, and the temperature range of its occurrence is broadened up to 600°C.

The values of the non-isothermal kinetic parameters are listed in Tables 1 and 2. A quite satisfactory agreement among the values obtained by help of the

Table 1 The non-isothermal kinetic parameters of the thermal decomposition of a CeO_2–Yb_2O_3 laser irradiated samples for 7 s with an energy density of 7.18 kJ·cm^{-2}

Method	E_a / cal·mol^{-1}	A / s^{-1}	Reaction order	Correlation coefficient
Coats–Redfern	9900	$1.79 \cdot 10^2$	1.20	0.99499
Flynn-Wall	10600	$8.79 \cdot 10^2$	1.10	0.99645
Modified Coats–Redfern	10600	$4.23 \cdot 10^2$	1.20	0.99559

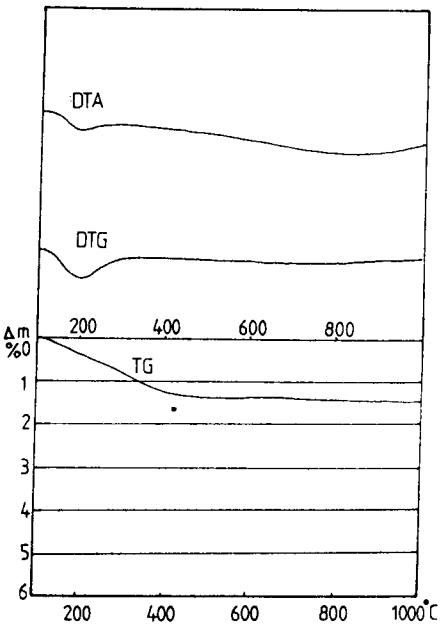

Fig. 3 Heating curves of CeO_2–5 wt.% Yb_2O_3 irradiated for 7 s and energy density of 16.15 kJ·cm^{-2}

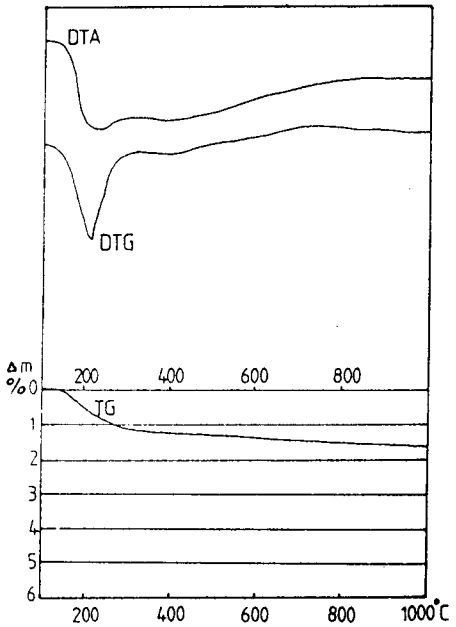

Fig. 4 Heating curves of CeO_2–5 wt.% Yb_2O_3 irradiated for 14 s and energy density of 7.18 kJ·cm^{-2}

Table 2 The non-isothermal kinetic parameters of the thermal decomposition of a CeO_2–Yb_2O_3 laser irradiated samples for 7 s with an energy density of 16.15 kJ·cm^{-2}

Method	E_a / cal·mol^{-1}	A / s^{-1}	Reaction order	Correlation coefficient
Coats–Redfern	6200	0.26	1.40	0.97799
Flynn-Wall	7300	4.76	1.30	0.98127
Modified Coats–Redfern	6700	0.59	1.40	0.97825

three applied methods has to be noticed. The fractional values of the reaction order are due to the contribution to the decomposition of structural units consisting of more than one molecule. Increase of the energy density of irradiation leads to a shift in the reaction order to 2 (Table 2).

TEM and SAED data

The reference sample (CeO_2 + 5% Yb_2O_3, calcined at 1000°C) exhibits the usual lines of pure stoichiometric CeO_2 with a_o = 5.41 Å (Figs 7a and 7b).

The characteristic diffraction pattern of the polycrystalline material does not show the lines of C–Yb_2O_3 (bcc) as the lines of this phase are superimposed on

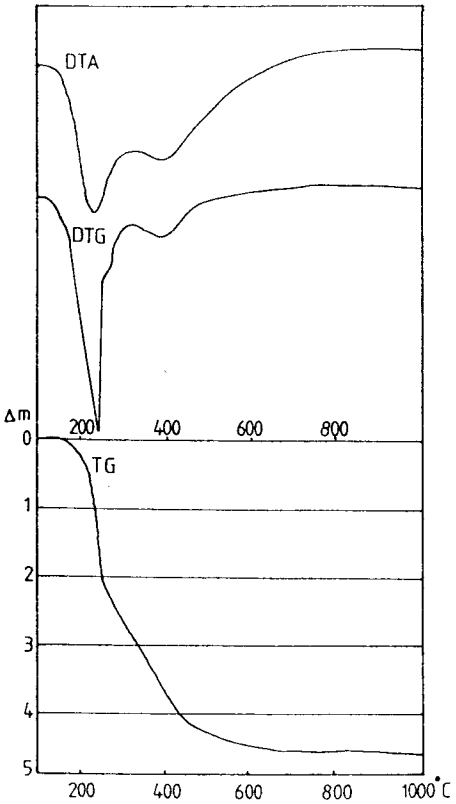

Fig. 5 Heating curves of CeO_2–5 wt.% Yb_2O_3 irradiated for 14 s and energy density of 10.77 kJ·cm^{-2}

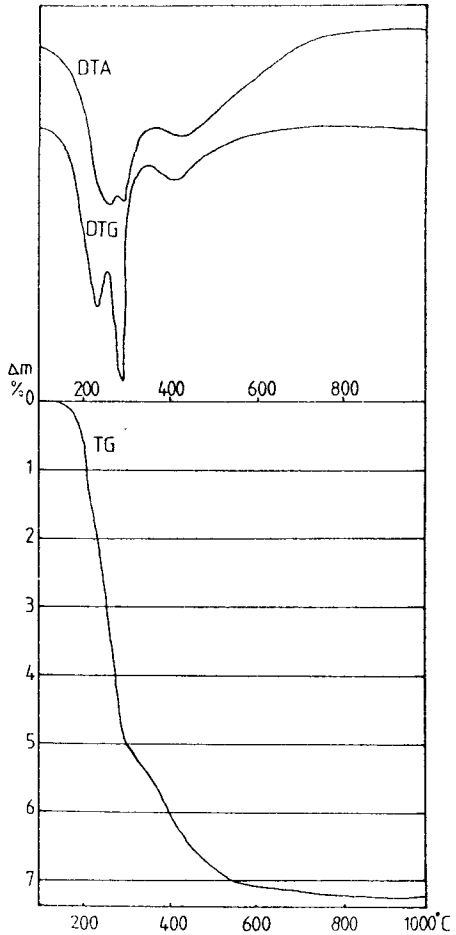

Fig. 6 Heating curves of CeO_2–5 wt.% Yb_2O_3 irradiated for 14 s and energy density of 16.15 kJ·cm^{-2}

the intense lines of CeO_2 (fcc). Nevertheless, some fine particles of C–Yb_2O_3 with [111] orientations were detected in the reference sample (Fig. 8).

The time of exposure and the energy density exert specific influences. The sample irradiated at 17.18 kJ·cm^{-2} for 7 s does not exhibit special structural effects, but only plaquetting effects. The plaques of stoichiometric CeO_2 exhibit low indices of orientation, such as [001] (Fig. 9) and [011] (Fig. 10), or relatively high indices, such as [114]. The orientation [011] seems to prevail.

The samples irradiated at 10.77 kJ·cm^{-2} contain monocrystalline CeO_2 particles with nonaltered stoichiometry and various morphologic habituses.

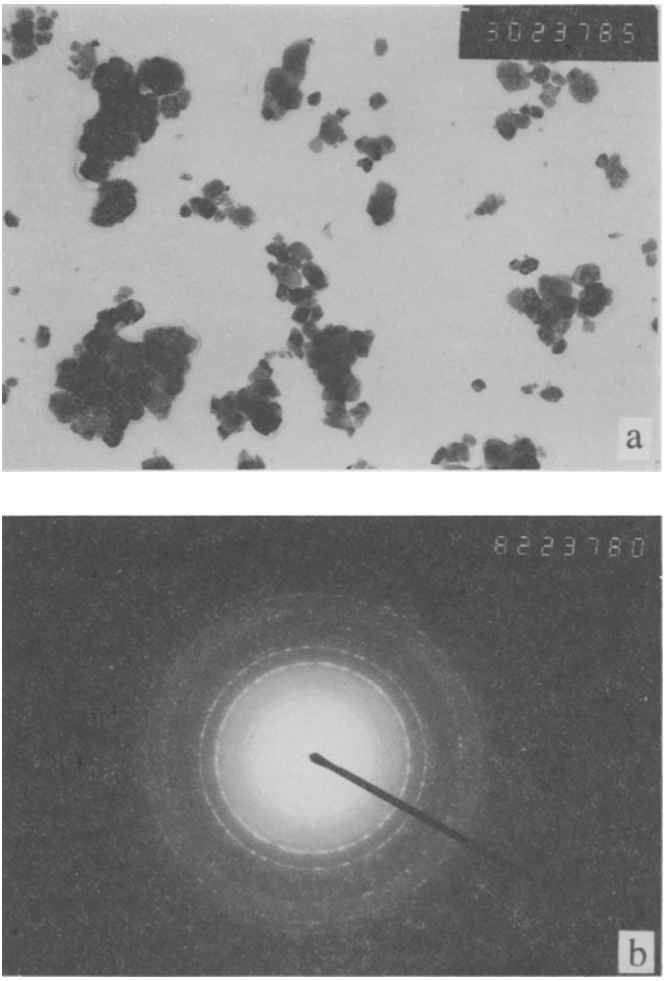

Fig. 7 TEM (a) and SAED (b) of CeO_2–5 wt. % Yb_2O_3 calcined at 1000°C

The samples exposed for 14 s gave different patterns at different radiation energy densities. Thus, the samples irradiated at 7.18 $kJ \cdot cm^{-2}$ exhibit a monoclinic phase close to B–Yb_2O_3 (Fig. 11) in a C–Yb_2O_3 particle with zone axis $<2,3,13>$.

This could not be indexed coherently. This is the reason for the possible assignment of this phase as belonging to the system of nonstoichiometric oxides CeO_{2-x}.

The microstructural investigations of these samples after heating in the derivatographic regime (10 $deg \cdot min^{-1}$ up to 600°C) did not reveal significant changes.

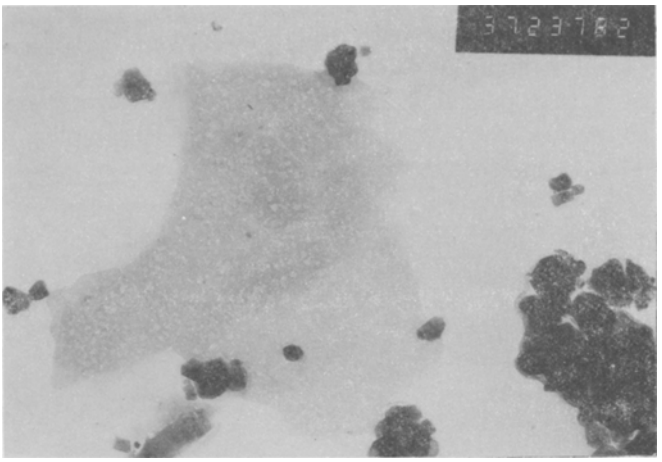

Fig. 8 TEM of CeO_2–5 wt.% Yb_2O_3 calcined at 1000°C

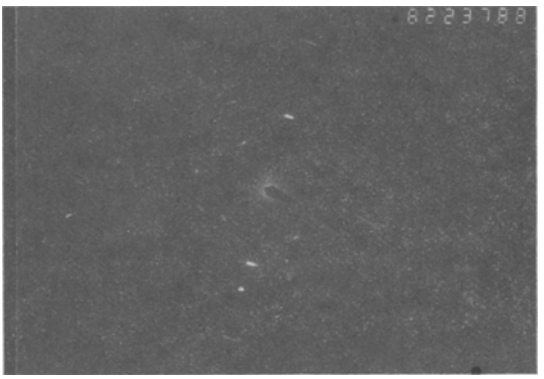

Fig. 9 SAED of CeO_2–5 wt.% Yb_2O_3 irradiated for 7 s and energy density of 17.18 $kJ \cdot cm^{-2}$

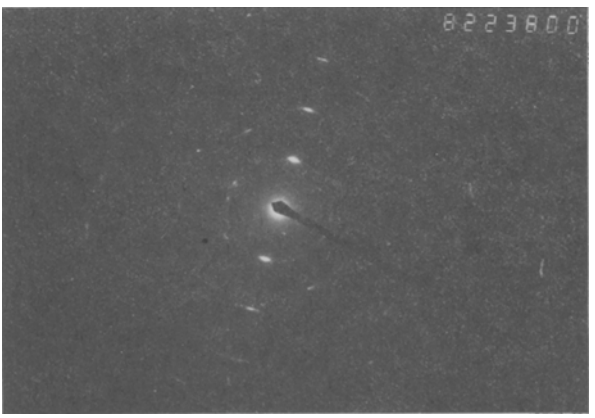

Fig. 10 SAED of CeO_2–5 wt.% Yb_2O_3 irradiated for 7 s and energy density of 17.18 $kJ \cdot cm^{-2}$

The samples laser-irradiated with energy densities higher than 10.18 $kJ \cdot cm^{-2}$ exhibit many monoclinic plaques that consist of stoichiometric CeO_2. The identified particles are characterized by zone axis <1,1,2> (Fig. 12). Calcination of these samples in the derivatographic regime led to CeO_{2-x} and B–Yb_2O_3 phases, as shown in Fig. 11.

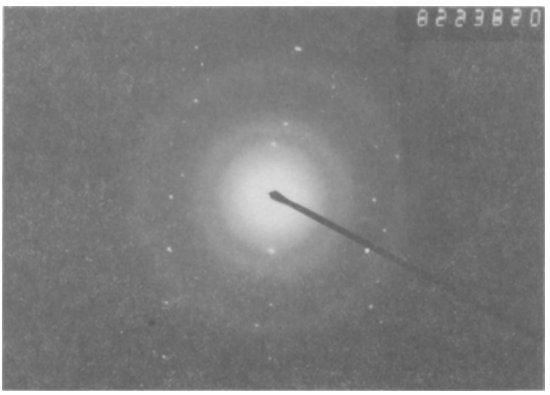

Fig. 11 SAED of CeO_2–5 wt.% Yb_2O_3 irradiated for 14 s and energy density of 7.18 $kJ \cdot cm^{-2}$

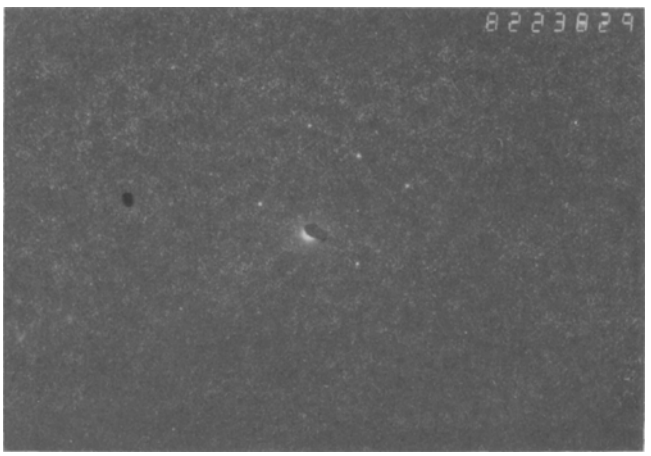

Fig. 12 SAED of CeO_2–5 wt.% Yb_2O_3 irradiated for 14 s and energy density of 10.18 $kJ \cdot cm^{-2}$

Discussion

The laser radiation energy density and the loss in mass observed derivatographically are closely correlated. Microstructural investigations showed that the samples irradiated at energy densities lower than 10 $kJ \cdot cm^{-2}$ exhibit non-

stoichiometric phases or particles with relatively high indices. The mass losses due to heating at temperatures below 400°C are lower than 2% and do not reflect important structural changes.

The samples irradiated at laser energy densities higher than 10 $kJ \cdot cm^{-2}$ for 14 s exhibit particles with nonaltered stoichiometry with respect to the reference samples. The derivatographic data on these samples showed losses in mass up to 7.2%. Structurally, the samples heated in the derivatographic regime are similar to those obtained on irradiation for short times. Thus, the phases generated by laser irradiation at energy densities lower than 10 $kJ \cdot cm^{-2}$ are stable and similar to those obtained by calcination at 1000°C. For a higher exposure time (t = 14 s), increase of the laser radiation energy density to values higher than 10 $kJ \cdot cm^{-2}$ leads to unstable stoichiometric phases which, on heating at 10 $deg \cdot min^{-1}$, decompose with mass losses, up to 7.2%. From this value, it can be concluded that in the new nonstoichiometric structures CeO_{2-x}, x attains values up to 0.8.

It can be stated that laser irradiation of CeO_2–Yb_2O_3 samples causes a reducing effect, observed for other oxide systems too [11] or for thin layers of rare-earth oxides irradiated with electrons [12–14]. Irradiation at high energy densities leads to the generation of monocrystalline plaques of stoichiometric CeO_2 stabilized by Yb^{3+} ions, which capture the anionic vacancies and allow the generation of nonstoichiometric phases belonging in the system CeO_{2-x}. On heating, these metastable particles of CeO_2 doped with Yb^{3+} decompose, thereby generating phases similar to those obtained on irradiation with low-energy density laser beams.

Conclusions

The CO_2 laser irradiation of CeO_2–Yb_2O_3 samples in continuous wave leads to structural changes that depend on the beam energy density and the exposure time.

Irradiation at high density energy generates metastable phases that probably lose oxygen up to the level of samples irradiated at low energy density, in which the reducing effect prevails.

A nonisothermal kinetic analysis was performed of the thermal decomposition of some irradiated samples.

References

1 S. R. Meech, Annual Reports C, The Royal Society of Chemistry, Cambridge 1988.
2 F. Curcio, G. Ghiglione, M. Musci and C. Nannetti, Appl. Surf. Sci., 36 (1989) 52.
3 J. D. Casey and J. S. Aggerty, J. Mater. Sci., 22 (1987) 4307.
4 F. Curcio, M. Musci, N. Notaro and G. de Michele, Appl. Surf. Sci., 46 (1990) 225.

5 V. Pârvulescu, A. Andrei and E. Segal, J. Thermal Anal., 44 (1995) 147.
6 C. Sârbu, V. Pârvulescu, F. Vasiliu and D. Bojin, Electron Microscopy, Vol. II, EUREM 92, Granada, Spain, 1992, p. 461.
7 A. W. Coats and J. P. Redfern, Nature (London), 201 (1964) 68.
8 J. H. Flynn and L. A. Wall, Polym. Lett., 4 (1966) 323.
9 E. Urbanovici and E. Segal, Thermochim. Acta, 81 (1984) 379.
10 N. Dragoe and E. Segal, Thermochim. Acta, 188 (1991) 305.
11 E. E. Khawaja, M. A. Khan, F. F. Al-Adel and Z. Hussain, J. Appl. Phys., 68 (1990) 1205.
12 L. Eyring, High Temp. Sci., 20 (1985) 183.
13 M. Gasgnier, G. Schiffmacher, L. Eyring and P. Caro, J. Less-Common. Met., 127 (1987) 167.
14 M. Gasgnier, G. Schiffmacher, D. Svoronos and P. Caro, J. Microsc. Spectrosc. Electron., 13 (1988) 13.

Zusammenfassung — Es werden Ergebnisse einer Untersuchung des thermischen Verhaltens von CeO_2-Proben dargelegt, die mit CO_2-Laser bestraht wurden.